

Network Design Considerations for Non-Topographic Photogrammetry

The problems of zero-, first-, second-, and third-order network design are addressed.

INTRODUCTION

IN PLANNING an optimal multi-station photogrammetric network for some special purpose, such as for monitoring structural deformation or for determining the precise shape characteristics of an object, due attention must be paid to the quality of the network design. Based on a given set of user accuracy specifications, quality is usually expressed in terms of the precision and reliability of the photogrammetric network, but it also may include aspects of economy and testibility (Schmitt, 1981). Precision is determined at the design stage as a function of the geometry of the network, i.e., its configuration and the precision of the measurements involved. The observables usually comprise

diagnosis is not considered. Aspects of network diagnosis as they relate to engineering surveying are well covered in Alberda (1980) and Niemeier (1982), and reliability considerations in close-range photogrammetry have been addressed by Grün (1978, 1980) and Torlegård (1980).

Following the classification scheme of Grafarend (1974), the interrelated problems of network design can be identified as

Zero-Order Design (ZOD): the datum problem,
First-Order Design (FOD): the configuration problem,
Second-Order Design (SOD): the weight problem, and
Third-Order Design (TOD): the densification problem.

By referring to the standard parametric model for the self-calibrating bundle adjustment, the different

ABSTRACT: *In the establishment of an optimal multi-station, non-topographic photogrammetric network, a number of tasks need to be carried out at the planning stage. Based on a given set of user accuracy requirements, the network must be designed, diagnosed, and, if necessary, optimized. The problem of optimal design can be classified in terms of four interconnected problems: zero-, first-, second-, and third-order design. Zero-order design embraces the datum problem, first-order design the configuration problem, second-order design the weight problem, and third-order design the densification problem. In this paper these four optimization components are discussed in the context of photogrammetric networks for non-topographic applications. Specific design characteristics are outlined, and these are demonstrated through network simulations.*

only image coordinates, but they may include measurements in the object space between target points and/or camera stations. Reliability is concerned with the control of quality of conformance of an observed network to its design. Thus, this aspect deals with network diagnosis or checking for model errors, e.g., systematic errors, outlying observations, and wrong functional relationships. The pursuit of optimal reliability, especially external reliability, is closely connected to the optimization of network precision. This paper addresses the tasks of photogrammetric network design and optimization, but

orders of design can be identified in terms of fixed and free quantities within the least-squares adjustment process (Schmitt, 1981). The linear functional and stochastic model can be written as

$$\begin{aligned} \mathbf{v} &= \mathbf{A}\mathbf{x} - \ell \\ \mathbf{C}_\ell &= \sigma_0^2 \mathbf{P}^{-1} \end{aligned} \quad (1)$$

where ℓ , \mathbf{v} , and \mathbf{x} are the vectors of observations, residuals, and unknown parameters, respectively; \mathbf{A} is the design or configuration matrix; \mathbf{C}_ℓ is the covariance matrix of observations; \mathbf{P} is the weight matrix; and σ_0^2 is the variance factor. In situations where \mathbf{A} is of full rank, i.e., redundant or explicit minimal constraints are imposed, the parameter estimates $\hat{\mathbf{x}}$

* Presently with Geodetic Services, Inc., 1511 River-view Drive, Melbourne, FL 32901

and the corresponding covariance matrix C_x are obtained as

$$\hat{x} = (A^T P A)^{-1} A^T P \ell = Q_x A^T P \ell$$

and

$$C_x = \sigma_0^2 Q_x \quad (2)$$

where Q_x is the cofactor matrix of the parameters. If A has a datum defect of rank, a Cayley inverse of the singular normal equations is not possible and some form of free-network approach employing implicit minimal constraints (e.g., through generalized inverses) is adopted. This aspect is covered in the section of the paper dealing with ZOD.

In the model, Equation 1, the parameters in x are treated as free unknowns, and for the following discussion it is assumed that prior information about the means and variances of these parameters has not been incorporated into the adjustment. However, the design procedures to be outlined certainly do not preclude the incorporation of prior parameter information, and where a weight matrix $P_{x,0}$ is available for the prior means x^0 , it can be entered into the least-squares model in the normal fashion. However, a few straightforward restrictions on the structure of $P_{x,0}$ do apply (Fraser, 1982).

The datum problem or ZOD involves the choice of an optimal reference system for the object space coordinates, given the photogrammetric network design and the precision of the observations. That is, for fixed A and P one usually seeks, through the selection of an appropriate datum, an optimum form of the cofactor matrix Q_x .

The configuration problem or FOD is concerned with the search for an optimal network geometry, given both the precision of the observations and criteria for the structure of the covariance matrix C_x of the parameters. This procedure thus entails the finding of an optimal design matrix A , given a weight matrix P , subject in certain cases to satisfying criteria imposed by a given Q_x or ideal covariance matrix. In non-topographic photogrammetry FOD embraces such aspects as camera and target point locations, imaging geometry, camera selection, and the influence of self-calibration in the final bundle adjustment. The most common approach to FOD is through network simulation, and such a process is adopted in this paper.

The weight problem or SOD involves the search for an optimal distribution of observational work, given both a network design and some ideal structure of C_x . This problem is characterized by an unknown P and fixed A and Q_x , i.e., by a solution to the matrix equation

$$(A^T P A)^{-1} = Q_x \quad (3)$$

In the area of geodetic networks, considerable research attention has recently been directed to the analytical solution of Equation 3 by both direct and indirect methods (Cross, 1981; Grafarend *et al.*,

1979). One feature of photogrammetric observations, however, impacts very favorably on the solution to the weight problem. In most practical applications, the structure of P is of the form $\sigma^{-2} I$ where σ^2 is a global measure of the variance of image coordinate measurements. Thus, SOD involves only the adoption of a suitable scalar value σ^2 for the weight matrix. Of course, in situations where the adopted P is either a block-diagonal matrix of 2×2 submatrices (Brown, 1980) or a more complex structure (Förstner and Schroth, 1981), the solution to the weight problem is not so straightforward. In this paper only the design case of $P = \sigma^{-2} I$ is considered.

The densification problem or TOD concerns the question of how best to enhance the precision of a network through the addition of extra object points and observations. Given an ideal Q_x , both A and P are updated to improve the network. Simulation, notably through the use of interactive computer graphics (Mephram and Krakiwsky, 1981), has proven a successful method for TOD in geodetic network design. As in SOD, the densification problem seems to be somewhat simplified for non-topographic photogrammetric networks. As will be shown in a later section of this paper, the impact on object point precision of adding additional points in an already "strong" network, as measured by the change in Q_x , is minimal.

The design problems outlined above are linked by a number of interrelated aspects. Nevertheless, the four classifications are widely accepted and the sequence is basically chronological. In the following sections each of the design problems is addressed in the context of analytical non-topographic photogrammetry. Throughout the discussion use is made of simulated close-range photogrammetric networks, which help in the illustration of important design concepts.

ZOD—THE DATUM PROBLEM

Unlike aerial triangulation, which represents a process of network densification, non-topographic photogrammetry is more often than not applied to network establishment. The difference between these processes is significant in the context of ZOD. Ackermann (1981) has pointed out that in aerial triangulation the datum problem is always solved; a ground control network is already in place. On the other hand, photogrammetric networks for non-topographic applications are often characterized by their independence from existing object space control frameworks.

The following dilemma then arises: It is usually required to express the spatial position of object points within a three-dimensional XYZ Cartesian coordinate system, but the observables (photo coordinates, and possibly object space distances, height differences, and angles) do not contain any information about the datum of this coordinate system,

other than perhaps its scale if spatial distances are observed. Thus, a datum must be defined by the imposition of constraints which establish the origin, orientation, and scale of the XYZ reference coordinate system. These constraints are said to be minimal when they introduce no information into the photogrammetric adjustment that has the potential of distorting the shape of the relatively oriented block. That is, after an absolute orientation to minimal control, e.g., two object points "fixed" in XYZ and a non-collinear point "fixed" in Z, the parameters of network shape, namely distance ratios and space angles, will remain unchanged.

Parameters of shape are determined solely as a function of the system observations, and they are invariant with respect to changes in the datum, or zero-variance computational base. Object space coordinates, however, relate to the datum, and thus when the minimal constraint is changed so one can expect the solution vector \hat{x} and the cofactor matrix Q_x to be altered. In situations where the datum is arbitrarily assigned, ZOD can be thought of as being the process of establishing a particular zero-variance computational base which, for a given network geometry, yields a cofactor matrix Q_x of the parameters (exterior orientation, object space, and additional parameters) which is "best" in some sense.

The parameters of primary interest in a photogrammetric block are usually the object point XYZ coordinates and functions of these coordinates, such as distances, volumes, etc. Also sought is the object point accuracy as measured by the precision and reliability of the network. Thus, in considering ZOD it is useful to seek only a "best" form for the cofactor matrix $Q_x^{(2)}$ which relates to either all the XYZ coordinates or a subset thereof. It must be remembered that $Q_x^{(2)}$ is not an estimable quantity, and significant changes in coordinate precision accompany changes in the reference coordinate system (Fraser, 1982).

The solution for x which is optimal in the sense of minimizing the mean variance $\bar{\sigma}_c^2$ of the object point coordinates is provided by a free-network adjustment that makes use of the pseudo-inverse of the singular normal equations, after the elimination of the exterior orientation and additional parameters (APs). Given that most fold-in algorithms employed for the solution of the normal equations in bundle block adjustment first eliminate the vector x_2 of object point coordinates, such a scheme can pose computational difficulties. An equivalent, more computationally attractive approach to this so-called "main" solution is the method of inner constraints (Blaha, 1971), which has recently been applied in close-range photogrammetry (Brown, 1982; Fraser, 1982; Papo and Perelmutter, 1982). In addition to yielding optimum mean object point precision

$$\bar{\sigma}_c^2 = \frac{\sigma_0^2}{3n} \text{tr } Q_x^{(2)} \rightarrow \text{minimum} \quad (4)$$

where n is the number of points, a minimum Euclidean norm of the object point coordinate corrections is obtained. The inner constraints need not apply to all object points, and the imposition of this implicit minimal constraint may simply refer to a chosen subset of the target array (three points is naturally the minimum number).

In view of the fact that the "main" solution yields minimum mean variance, one may validly ask whether this free-network approach provides a solution to the datum problem. For numerous applications it may, and in the case of relative deformation networks (all points assumed unstable) free-network adjustment is advantageous (Fraser, 1983). But, much depends on the criteria set for $Q_x^{(2)}$ at the ZOD stage. For example, the common, computationally simpler approach of "fixing" object point coordinates to remove the seven (six if distances are observed) network defects of translation (three), rotation (three), and scale (one) will yield a mean variance $\bar{\sigma}_c^2$ for the object points, which is larger in magnitude than that obtained from the inner-constraints adjustment. Differences in the precision of parameters (e.g., distances) derived from \hat{x}_2 may, however, be insignificant from a practical point of view.

Through the use of an S-transformation, introduced by Baarda (1973), it is always possible to transform both \hat{x}_2 and $Q_x^{(2)}$ relating to one zero-variance computational base into their corresponding values for any other minimal constraint. For example, after the cofactor matrix of object point XYZ coordinates is computed for a datum of seven explicitly fixed coordinate values, the corresponding "main" solution for $Q_x^{(2)}$ is obtained simply by applying an S-transformation. Although the implementation of covariance transformations is relatively straightforward (Strang Van Hees, 1982), the S-transformation does necessitate the computation of a full $Q_x^{(2)}$ matrix. Thus, for close-range photogrammetric networks with dense target arrays, where a full covariance matrix may not be sought, it is often computationally more practical to readjust the network with a different datum rather than apply an S-transformation. The S-transformation is very applicable, however, when it is required to transform an ideal covariance matrix of XYZ coordinates into one which corresponds to a specific zero-variance computational base.

The impact on object point precision of changes in the minimal constraint configuration has been previously illustrated by Fraser (1982). Simulated network examples which demonstrate the need for a careful ZOD are now considered. Figure 1 shows a three-dimensional array of 27 targets, the corner points forming a cube with sides of 2 metres. This array is imaged by both "normal" and convergent four-photo configurations, each symmetric about the Z-axis through the center point of the target array. An angle of 60° is subtended by the optical

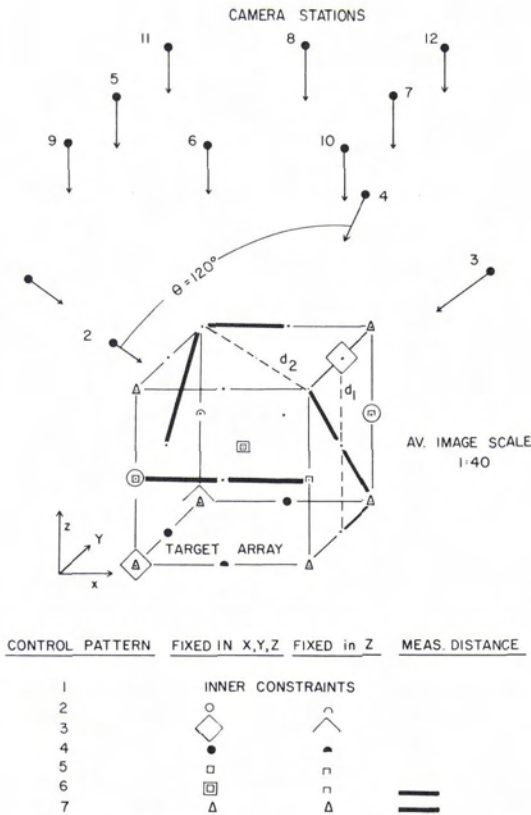


FIG. 1. Simulated object target array, with camera station positions and control configurations.

axes of each of the four camera stations forming the convergent network and the Z-axis (i.e., angle of convergence of $\theta = 120^\circ$), and the base/distance (B/D) ratio for the "normal" configuration (photos 5, 6, 7, and 8) is 0.8. The average imaging scale in each case is 1:40, i.e., exposure stations 4 m from the cube's center, and a camera focal length of 100 mm.

For the practical examination of the datum problem reported, seven object space constraint configurations have been considered: four minimal; two minimal with respect to translation and orientation, but redundant in scale information; and one redundant pattern of six fixed points in X, Y, and Z. These zero-variance computational bases are indicated in the legend of Figure 1. For each datum considered, the cofactor matrix $Q_x^{(2)}$ is obtained from the appropriate design matrix A and the weight matrix P , i.e.,

$$Q_x = \begin{pmatrix} \cdot & \cdot & \cdot \\ \cdot & Q_x^{(2)} & \cdot \\ \cdot & \cdot & \cdot \end{pmatrix} = \begin{pmatrix} A_1^T P A_1 & A_1^T P A_2 & 0 \\ A_2^T P A_1 & A_2^T P A_2 & G \\ 0 & G^T & 0 \end{pmatrix}^{-1} \quad (5)$$

for the network subject to inner constraints, and

$$Q_x = \begin{pmatrix} \cdot & \cdot \\ \cdot & Q_x^{(2)} \end{pmatrix} = \begin{pmatrix} A_1^T P A_1 & A_1^T P A_2 \\ A_2^T P A_1 & A_2^T P A_2 \end{pmatrix}^{-1} \quad (6)$$

for the remaining six cases. In Equations 5 and 6, the subscript 1 refers to exterior orientation and additional parameters, and 2 refers to object point coordinates. The matrix G is a Helmert transformation matrix (Blaha, 1971; Granshaw, 1980; Fraser, 1982), and for the simulations conducted $P = \sigma^{-2} I$, where $\sigma = \pm 3 \mu\text{m}$. Each " \cdot " represents a submatrix of the cofactor matrix, which is not pertinent to the present discussion.

From the $Q_x^{(2)}$ matrices obtained, Table 1 has been compiled. This table lists the mean standard error $\bar{\sigma}_c$ of the 27 object points; the mean standard errors $\bar{\sigma}_{XY}$ and $\bar{\sigma}_Z$ for the XY and Z coordinates; the standard errors σ_{d_1} and σ_{d_2} of the two distances indicated by dashed lines in Figure 1; the standard error ranges $\Delta\sigma_{XY}$ and $\Delta\sigma_Z$; and the factor q derived from the approximate formula

$$\bar{\sigma}_c \approx q S \sigma \quad (7)$$

where S is the scale number (40 in this case). Equation 7 can be used effectively as a coarse indicator of object point accuracy at the initial network design stage. For "strong" networks of three or more photographs, values in the range of $0.5 < q < 1.2$ can usually be anticipated. The standard error ranges $\Delta\sigma_{XY}$ and $\Delta\sigma_Z$ are indicators of the homogeneity of object point precision. If a near-homogeneous standard error distribution is sought, then $\Delta\sigma_{XY}$ and $\Delta\sigma_Z$ should be as small as possible. For this experiment the individual ranges in "planimetry," $\Delta\sigma_{XY}$, and "height," $\Delta\sigma_Z$, have been quoted, rather than $\Delta\sigma_{XYZ}$, principally because of the symmetric imaging geometries considered.

In the results presented in Table 1 the following characteristic features relating to ZOD can be recognized:

- Changes in minimal control not only influence the magnitude of object point coordinate standard errors, but also the degree of homogeneity of the network precision. In this regard, inner constraints provide a "best" solution, in addition to yielding maximum mean precision (minimum $\bar{\sigma}_c$).
- In both the "normal" and convergent configurations, the free-network adjustment yields higher mean precision than that obtained in the networks with either redundant coordinate control or point-to-point distance observations. This is an important property given that the establishment of other than an arbitrary minimal constraint requires extra surveying work. Note that a further inner constraint approach, which has not been employed here, can be used in conjunction with measured distances. Under this scheme the transformation matrix G has one column suppressed, that relating to the network defect of scale. Where distances are treated as observables (one having zero-variance) the resulting standard errors of point-to-point distances in the adjusted network become estimable quantities, i.e., they remain invariant with changes in

TABLE 1. VARIATIONS IN OBJECT POINT PRECISION WITH CHANGES IN THE CONTROL CONFIGURATION. THE UNITS OF σ -VALUES ARE mm.

object space control pattern	q	$\bar{\sigma}_c$	$\bar{\sigma}_{XY}$	$\bar{\sigma}_Z$	$\Delta\sigma_{XY}$	$\Delta\sigma_Z$	σ_{d_1}	σ_{d_2}
<i>convergent</i>								
1.	0.6	0.07	0.07	0.07	0.01	0.03	0.10	0.09
2.	0.9	0.11	0.11	0.11	0.03	0.06	0.13	0.15
3.	1.0	0.12	0.12	0.10	0.07	0.05	0.11	0.14
4.	1.1	0.14	0.14	0.13	0.12	0.12	0.12	0.24
5.	0.9	0.11	0.11	0.10	0.05	0.08	0.12	0.10
6.	1.1	0.14	0.15	0.13	0.07	0.09	0.12	0.10
7.	0.7	0.08	0.08	0.08	0.01	0.03	0.11	0.11
<i>"normal"</i>								
1.	0.9	0.11	0.07	0.16	0.03	0.12	0.26	0.16
2.	1.5	0.18	0.14	0.24	0.08	0.24	0.31	0.15
4.	3.0	0.37	0.37	0.38	0.45	0.34	0.32	0.27
5.	1.5	0.18	0.15	0.23	0.12	0.16	0.29	0.13
7.	1.0	0.12	0.08	0.14	0.04	0.15	0.27	0.11

the minimal constraints of orientation and translation. This is indicated in the table by the standard errors σ_{d_1} and σ_{d_2} which are the same for control patterns 5 and 6 in the convergent case. Although not indicated in Figure 1, configurations 5 and 6 have an additional Y coordinate fixed to remove the third orientation defect (rotation about the Z-axis).

- An "optimum" minimal control configuration of two points fixed in XYZ and one fixed in Z (or X or Y) is likely to be approached when the centroid of the triangle formed by the three object control points is reasonably close to the target array center and the triangle's area is a maximum. For example, compare the results for control patterns 2, 3, and 4. Pattern 2 can be thought of as a favorable minimal control configuration, whereas pattern 4 is, as expected, very unfavorable.
- For favorable minimal control configurations, the variation in the precision of certain functions of $Q_x^{(2)}$, which accompany changes in the datum, can be expected to be somewhat less than the variation in $\bar{\sigma}_c$. This is notably the case with distances, as is indicated for patterns 1, 2, and 3 in Table 1.

In concluding this section on ZOD, the point must be made that the datum problem is not independent of the configuration problem. The extent to which a change in datum will influence object point precision is very much dependent on imaging geometry. For the two imaging geometries considered, a change in the zero-variance computational base seems to influence the precision of the "normal" network to a greater degree than the convergent, especially in the case of an unfavorable minimal constraint such as pattern 4.

FOD—THE CONFIGURATION PROBLEM

For non-topographic photogrammetric networks, FOD primarily involves the choice of an appropriate imaging geometry for a given array of object target points. The aim here is to find a configuration matrix

A which, for a given weight matrix P, yields a cofactor matrix $Q_x^{(2)}$ which meets specified criteria. For example, a criterion may be that $Q_x^{(2)}$ has a structure which is both homogeneous and isotropic, i.e., all point error ellipsoids are spheres of equal radius. However, it is well known that a "normal" imaging configuration cannot yield an isotropic form of $Q_x^{(2)}$ and convergent multi-station photography would therefore be required in this case. This does not imply that "normal" imaging should be rejected out of hand, as the criteria for optimum precision may call for a covariance matrix which is other than homogeneous and isotropic (Fraser, 1983).

Although its principal component is imaging geometry, FOD also embraces a number of the well-recognized methods for enhancing object point precision. These include the adoption of larger image scales and long focal length photography, the use of target clusters around an object point, and multiple exposures at each camera station. The latter aspect can also be interpreted as a component of the second-order or weight problem, much like the multiple measurement of image coordinates. Also, in terms of optimizing precision (but not necessarily reliability), the use of target clusters can be considered as part of the TOD process. A further important aspect of the configuration problem is the influence of APS—be they block-invariant or sub-block invariant, coefficients of general polynomial functions, or physically interpretable camera calibration parameters—on the precision of object point determination. The following papers address various accuracy enhancement approaches which can be classified as part of the FOD procedure: Kenefick (1971), Hottier (1976), Grün (1978, 1980), Fraser (1980), Brown (1980), Granshaw (1980), and Veress and Hatzopoulos (1981). In discussing the configuration problem, it is useful to consider the above mentioned aspects under separate headings.

IMAGING GEOMETRY

As the central component of FOD, the selection of an appropriate imaging geometry for a multi-station photogrammetric network deserves close examination. In this section the impact of six different imaging configurations on the object point precision of the 27-point target array shown in Figure 1 is examined. Two of the imaging arrangements are "normal," one a mixture of "normal" and convergent, and three convergent. All networks employ four photographs, with a datum defined by means of the use of inner constraints, thus leading to a covariance matrix $C_x^{(2)}$ with minimum trace. For the "normal" geometries, a B/D ratio of 0.8 has been adopted, and for the four stations 1, 2, 3, and 4, which are symmetrically disposed about the cube as shown in Figure 1, convergence angles of 60° , 120° and 180° have been considered.

Prior to examining the results of the FOD simulations, which are presented in Table 2, one aspect regarding the use of a convergent geometry needs to be recalled. Simulations conducted by Kenefick (1971), Brown (1980), and Granshaw (1980), among others, have clearly indicated the significant overall accuracy enhancement that can be anticipated through the use of convergent rather than "normal" photography. However, there are recent reports that at first sight appear to contradict these findings (Schwartz, 1982; El-Beik and Babaei-Mahani, 1982). It is more than likely that if a fall-off in accuracy accompanies the employment of increasingly large convergence angles, then this is due to errors in the calibration of the interior orientation elements x_0 , y_0 , and f . By carrying these parameters as additional system unknowns in a network of suitable geometry, this problem can be alleviated.

In numerous practical applications, the site of a photogrammetric survey can impose restraints on the selection of an ideal imaging geometry, especially in industrial photogrammetry. Thus, the adoption of a less than optimal imaging geometry is frequently necessary in practice. This limitation should be kept in mind when examining the results in Table 2; they refer to only six rather idealized networks. Nevertheless, from the table a number of generally

applicable observations can be made, and these include

- The well-known discrepancy between $\bar{\sigma}_{XY}$ and $\bar{\sigma}_Z$ for "normal" networks is illustrated for configurations 1 and 2, with the effect being more pronounced in the second case. Further comments on this aspect are made in the following section on the influence of changes in the B/D ratio. With respect to the X and Y coordinates only, a very homogeneous distribution of precision is attained, as is expected from the symmetry of the imaging geometry.
- Whereas the combination of two "normal" and two convergent camera stations does not influence $\bar{\sigma}_{XY}$ to a significant degree, $\bar{\sigma}_Z$ and therefore $\bar{\sigma}_c$ are reduced significantly. Changes in $\bar{\sigma}_Z$ are directly proportional to changes in the convergence angle θ , which is 120° in the case of configuration 3.
- Of the three convergent imaging geometries, the configuration with $\theta = 120^\circ$ gives both a near-isotropic form of $Q_x^{(2)}$ and a very homogeneous distribution of object point accuracy. This homogeneity is reflected in the precision of point-to-point distances, the standard errors being essentially independent of distance. For the majority of three-dimensional measuring tasks, such results would constitute a "best" solution to the imaging geometry problem of FOD.
- Of the networks considered, the one yielding the most homogeneous distribution of object point accuracy, as measured by $\Delta\sigma_{XY}$ and $\Delta\sigma_Z$, is that with a convergence angle of 180° . Such a symmetric imaging geometry, albeit using only three camera stations, has been employed by Gates *et al.* (1982) in the calibration of three-dimensional measuring machines.
- As regards the precision of object space distances, volumes, coordinate differences, etc., it will generally be found that an optimal design calls for a reasonably homogeneous distribution of object point coordinate accuracy. Functions which are restricted to either one or two dimensions (e.g., distances in the XY plane) are, however, obvious exceptions to this rule.

It is the author's view that the important information contained in Table 2, as far as FOD is concerned, is not so much the magnitudes of the $\bar{\sigma}_c$ or q values listed, but more the relationship between $\bar{\sigma}_{XY}$ and $\bar{\sigma}_Z$ (or $\bar{\sigma}_X$, $\bar{\sigma}_Y$, and $\bar{\sigma}_Z$). In the first instance an im-

TABLE 2. THE INFLUENCE OF VARIATIONS IN IMAGING GEOMETRY ON OBJECT POINT PRECISION. THE UNITS OF σ -VALUES ARE mm.

imaging configuration	q	$\bar{\sigma}_c$	$\bar{\sigma}_{XY}$	$\bar{\sigma}_Z$	$\Delta\sigma_{XY}$	$\Delta\sigma_Z$	σ_{d_1}	σ_{d_2}
1. "normal" (stns. 9-12)	0.7	0.09	0.07	0.12	0.03	0.09	0.18	0.11
2. "normal" (stns. 5-8)	1.0	0.12	0.08	0.17	0.03	0.12	0.26	0.16
3. "normal" + convergent (stns. 2, 4, 5, 7)	0.6	0.07	0.07	0.09	0.01	0.05	0.13	0.09
4. convergent, $\theta = 60^\circ$	0.8	0.09	0.07	0.13	0.02	0.09	0.20	0.11
5. convergent, $\theta = 120^\circ$	0.6	0.07	0.07	0.07	0.01	0.03	0.10	0.10
6. convergent, $\theta = 180^\circ$	0.6	0.07	0.08	0.06	0.01	0.01	0.08	0.09

aging geometry should be sought which satisfies the specified homogeneity criteria for $Q_x^{(2)}$. The absolute value of $\bar{\sigma}_c$ can be scaled down through further FOD processes and in the SOD stage, but the fundamental distribution of relative object point and point coordinate accuracies is established once the imaging geometry is in place.

BASE/DISTANCE RATIO

For the "normal" networks examined in the previous sections only a B/D ratio of 0.8 (in both the X and Y directions) was considered. However, it is well established that an increase in the B/D ratio is accompanied by both an improved level of mean object point precision (Hottier, 1976) and enhanced reliability (Grün, 1978, 1980). To illustrate the impact on FOD of changes in the B/D ratio, the camera station geometry indicated by configuration 1 in Table 2 is examined. Table 3 lists the mean standard errors corresponding to three adopted B/D ratios of 0.6, 0.8, and 1.0 for this network. It is apparent from the results presented in the table that $\bar{\sigma}_c$ falls off in value non-linearly as the base decreases. The deterioration in precision, principally in the Z -direction, comes about because of the less favorable ray intersection geometry which accompanies small B/D ratios. A decrease in the B/D ratio from 1.0 to 0.6 is accompanied by an increase in $\bar{\sigma}_z$ of 0.07 mm, or a reduction in precision of about 80 percent. Due to the restrictive geometry of a "normal" network, alterations in the B/D ratio provide one of the few means for enhancing the distribution of object point precision.

NUMBER OF CAMERA STATIONS

The practice of using multi-station photogrammetric networks, as opposed to single stereopair configurations, is well established in precision non-topographic photogrammetry. Depending on the imaging geometry adopted, the use of additional camera stations can be expected to not only improve precision, but also to significantly enhance the network's reliability. An examination of accuracy improvements which accompany the use of an increasing number of exposure stations cannot, however, be divorced from a consideration of the corresponding changes in imaging geometry. Additional imaging rays increase the redundancy in a spatial intersection, and also alter the intersection geometry.

Notwithstanding the difficulties of considering in isolation the influence on FOD of the number of camera stations, one general observation that can be made is that for "strong" networks, the accuracy improvement obtained over a two-photo geometry is approximately proportional to $m^{1/2}$, where m is the number of photographs. This implies that, if the number of camera stations is increased from two to three, a significant improvement in object point precision can be expected, whereas a change from three to four photos is only likely to decrease $\bar{\sigma}_c$ by about 20 percent. The inverse proportionality between $\bar{\sigma}_c$ and $m^{1/2}$ only holds approximately, however, and is not applicable to all network designs.

To illustrate the effect on object point precision of incorporating extra camera stations, the target field and camera stations shown in Figure 1 are again considered. Table 4 lists the mean object point coordinate standard errors that are obtained from imaging configurations of two, three, four, six, and eight photographs, the datum for each adjustment being defined by means of the "main" solution. As anticipated, when three camera stations are employed rather than two, the results indicate a significant improvement in both the magnitude and homogeneity of object point precision. However, increasing the coverage from four photos to eight reduces the value of $\bar{\sigma}_c$ by less than 20 μm or 1/200,000th of the imaging distance. With these results in mind, it seems reasonable to assert that in the FOD process more attention should be paid to the imaging geometry, rather than concentrating too much on obtaining a coverage of a certain arbitrary number of photographs, with the restriction of course that a minimum of three intersecting rays (not in the same epipolar plane) at each object point is very desirable.

MULTIPLE EXPOSURES

The use of multiple exposures at a camera station provides a practical means of enhancing network accuracy. In situations where successive exposures cannot be assumed to be taken at precisely the same orientation and position, an additional set of exterior orientation parameters is introduced into the network for each successive photograph. Thus, at the design stage A is modified and so the process of selecting how many exposures should be taken becomes one of FOD. However, if the same number of exposures, k , is taken at each camera station, the

TABLE 3. OBJECT POINT PRECISION OBTAINED FOR A FOUR-PHOTO "NORMAL" NETWORK WITH THREE B/D RATIOS. THE UNITS OF σ -VALUES ARE mm.

B/D ratio	q	$\bar{\sigma}_c$	$\bar{\sigma}_{XY}$	$\bar{\sigma}_z$	$\Delta\sigma_{XY}$	$\Delta\sigma_z$	σ_{d_1}	σ_{d_2}
0.6	0.9	0.11	0.07	0.16	0.03	0.12	0.25	0.15
0.8	0.7	0.09	0.07	0.12	0.03	0.09	0.18	0.11
1.0	0.6	0.07	0.06	0.09	0.03	0.08	0.14	0.10

TABLE 4. THE INFLUENCE OF THE NUMBER OF CAMERA STATIONS ON OBJECT POINT PRECISION. THE UNITS OF σ -VALUES ARE mm.

number of camera stations	q	$\bar{\sigma}_c$	$\bar{\sigma}_x$	$\bar{\sigma}_y$	$\bar{\sigma}_z$	$\Delta\sigma_{xy}$	$\Delta\sigma_z$
2 (#1 and 3)	1.1	0.13	0.17	0.09	0.11	0.10	0.05
3 (#1 to 3)	0.7	0.08	0.09	0.08	0.08	0.02	0.05
4 (#1 to 4)	0.6	0.07	0.07	0.07	0.07	0.01	0.03
6 (#1 to 5 and 7)	0.5	0.06	0.05	0.05	0.06	0.01	0.03
8 (#1 to 8)	0.4	0.05	0.05	0.05	0.06	0.01	0.03

influence on network precision is essentially equivalent to adjusting the single-exposure configuration with a weight matrix $P_k = kP$. The cofactor matrix is then obtained as

$$Q_{xk} = (A^T P_k A)^{-1} = k^{-1} (A^T P A)^{-1} = k^{-1} Q_x \quad (8)$$

where Q_x corresponds to one photograph per station, and Q_{xk} to k exposures per camera station. Leading directly from Equation 8 are the relationships

$$\bar{\sigma}_{c_k} = k^{-1/2} \bar{\sigma}_c \quad \text{and} \quad q_k = k^{-1/2} q. \quad (9)$$

Because the use of multiple exposures leads to simply a scaling of the weight matrix P , the process can be considered as a component of SOD, and further remarks will be made on this design aspect in the section dealing with the weight problem.

NUMBER OF POINTS

In bundle adjustments of well designed photogrammetric networks, which do not incorporate self-calibration, the number of object points has surprisingly little impact on the mean standard error $\bar{\sigma}_c$. Consider, for example, the two- and three-photo convergent networks indicated in Table 4. An increase in the number of target points from 27 to 45 results in a reduction in the value of $\bar{\sigma}_c$ of less than 10 μm for both networks. Further, if the number of points is reduced to 15, a similarly insignificant change in network precision results. Due to the practical independence of object point precision and the number of target points, networks which are planned to include hundreds of points can be examined and optimized at the FOD stage by considering only say 20 to 40 well distributed targets. This leads to considerable savings in the computation of a representative $Q_x^{(2)}$.

Whereas the accuracy attained in a standard bundle adjustment is not significantly influenced by the number of target points, the precision yielded in a self-calibration adjustment is considerably affected by both the density and distribution of the object points. In the majority of systematic error compensation models employed for self-calibration,

the coefficients of the APs are expressed as functions of the image coordinates. The self-calibration process can be thought of as a surface fitting problem, albeit one which is not independent of photogrammetric resection and intersection. Consider, for example, lens distortion. The distortion pattern of a lens is quantified by the resulting image point displacements at the film plane. Thus, if a function is required to describe this pattern throughout the entire frame format, image points will need to be sufficiently well distributed on the film, and this in turn impacts on the distribution and number of object points imaged.

TARGET CLUSTERS

The use of clusters of targets rather than a single object point has been proposed as a practical means of enhancing network accuracy (Hottier, 1976; Torlegård, 1980). In the presence of local systematic error influences in the imaging and measuring systems, such an approach has its merits. For example, the ability to locate observation outliers (i.e., the internal reliability) can be expected to be enhanced by using target clusters. However, for favorable imaging geometries, the influence on object point precision of an increase in the number of targets, be they clustered or otherwise, is typically insignificant. At the FOD stage, therefore, the use of target clusters generally need not be considered in a network simulation, as a representative $Q_x^{(2)}$ can be derived through the use of single-point targets.

IMAGE SCALE AND FOCAL LENGTH

Basically, there is a linear relationship between object point precision (as expressed by $\bar{\sigma}_c$) and imaging scale, as indicated by Equation 7. An alteration in photographic scale can, however, modify the imaging geometry to a small extent, and thus changes in the scale number S and the mean standard error $\bar{\sigma}_c$ may not be exactly proportional. For the purposes of FOD, Equation 7 is generally sufficiently applicable.

Whereas an alteration in image scale may have only a scaling effect on $Q_x^{(2)}$, a change in focal length

(retaining the same mean photographic scale) can influence the distribution of precision in the object space. As the focal length of the taking camera increases, so the geometry of multi-ray intersections tends to become more homogeneous, thus leading to a reduction in the range of object point standard errors. For the four-photo convergent network shown in Figure 1, a change in focal length from 60 to 200 mm is accompanied by a reduction in $\Delta\sigma_{XY}$ from 0.021 to 0.003 mm, and in $\Delta\sigma_Z$ from 0.058 to 0.015 mm. Coupled with the enhancement of the homogeneity of object point precision, a further benefit of long focal length cameras is that they are less subject to the critical influence of film unflatness (Kenefick, 1971). At the network design stage the latter of these two features is perhaps the most important to keep in mind, although the choice of focal length is most often limited by both camera availability and the physical layout of the survey site. In general, this FOD aspect does not play an important role in network design or optimization.

SELF-CALIBRATION PARAMETERS

In recent years a considerable amount of research attention has been directed to the relationship of APs and network precision (Grün, 1978, 1980; Brown, 1980; Fraser, 1980, 1982). Due to the numerous additional parameter models applied and the various special considerations that are warranted when APs are sub-block invariant, photo-invariant, or a combination of these, it is difficult to establish general rules that will be effective in FOD. Nevertheless, a few characteristics of self-calibrating bundle adjustments warrant attention.

The first feature worth noting is that, in the presence of high intercorrelations between APs, and strong projective coupling between APs and exterior orientation elements, object point precision, and reliability are liable to be degraded. High correlation comes about through over-parameterization, e.g., polynomial terms of too high an order and the inclusion of APs which are not statistically significant. Care must be exercised in simulating networks which are to be adjusted by self-calibration. For example, if it required to examine the influence on $Q_x^{(2)}$ of carrying both interior orientation and decentering distortion parameters—which are often highly correlated—it is necessary to simulate an appropriate distortion pattern. In an examination of how well a distortion pattern can be modeled, the "error surface" must be input into the photogrammetric system.

As regards network geometry, it is well recognized that the determination of statistically significant APs is dependent on the provision of both a suitable imaging configuration and an adequate distribution of object points. For example, the recovery of the interior orientation parameters x_0 , y_0 , and f in a "normal" network requires a target point array which is well distributed in three dimensions,

and it is always enhanced by having non-constant (preferably mutually orthogonal) kappa rotations. As a rule, object point precision is not degraded so long as all APs are statistically significant. A further characteristic, which does not apply to standard bundle adjustments, is that the precision of APs is generally enhanced, along with the structure of $Q_x^{(2)}$, as the density of the object target point array is increased.

SOD—THE WEIGHT PROBLEM

In the photogrammetric case where $P = \sigma^{-2} I$, the weight problem involves only an optimization of the scalar value σ . There are effectively three methods available for increasing the precision of image coordinate observations: the use of a higher-precision comparator, multiple image coordinate measurements, and the use of multiple exposures, as outlined in the discussion on FOD. Because most high-precision photogrammetric surveys employ comparators with accuracies in the range of 1 to 2.5 μm , there is typically not much flexibility afforded in the selection of a comparator as far as SOD is concerned.

Of the two remaining approaches, the use of multiple exposures is, in the author's opinion, a more effective means of scaling σ to some required value. In theory, the effect on $Q_x^{(2)}$ of observing an image point k times is equivalent to a single observation of that point on each of k images taken at the same exposure station. However, the latter approach has one distinct advantage, that being that systematic error components which change from exposure to exposure (e.g., film deformation) are averaged over the k images. It is also possible, of course, to combine the two methods, e.g., multiple readings on each of the multiple exposures.

Figure 2 illustrates the reduction in the magnitude of $\bar{\sigma}_c$ which accompanies the use of multiple exposures for four networks: a two-photo "normal" configuration (exposures #5 and 7 in Figure 1), and the two-, three-, and four-photo convergent networks considered in Table 4. The change in object point accuracies can be completely represented by changes in $\bar{\sigma}_c$ because the same scale factor applies to the variances and covariances of $Q_x^{(2)}$, and relative

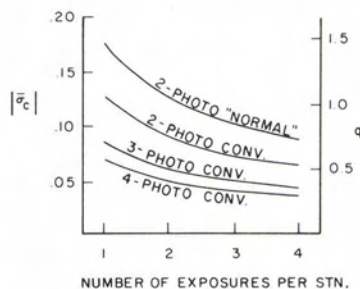


FIG. 2. The influence on object point precision of taking multiple exposures at each camera station.

precision is therefore not influenced. An experiment conducted by the author on the use of constraint functions of the form $\hat{x}_1^{(i)} - \hat{x}_1^{(i+1)} = 0$, where $\hat{x}_1^{(i)}$ is the vector of exterior orientation parameters for the i^{th} exposure at a camera station, did not result in an improvement in object point precision, though it is thought that such an approach may enhance the accuracy of networks employing non-metric cameras.

TOD—THE DENSIFICATION PROBLEM

In light of the fact that object point precision is largely independent of target array density in networks with "strong" geometries, the densification problem does not seem to arise. Effectively, the densification problem is solved at the FOD stage, and TOD generally need not be separately considered in a photogrammetric network optimization.

DESIGN THROUGH SIMULATION

Computer simulation of non-topographic photogrammetric networks has been successfully employed in design optimization for some time. But the development of powerful minicomputers and graphics terminals has given a considerable boost to interactive network design, to the point where simulation and adjustment software packages are becoming commercially available (Brown, 1982). The process of photogrammetric network design optimization through computer simulation can follow a number of approaches. One practical procedure is summarized by the flow diagram shown in Figure 3. Once the accuracy specifications have been es-

tablished, an observation and measuring scheme is adopted. This procedure may entail the selection of a particular camera or cameras for the survey, the comparator to be used, a first approximation of the imaging geometry, e.g., four-photo convergent configuration with scale 1:5, and all points appearing on all images. Equation 7 can prove very useful in this process. Appropriate values of the factor q are usually selected on the basis of results obtained in previous network designs. Alternatively, a coarse estimate for q could be based on the object point precision obtained in the networks considered in this paper.

Following the establishment of a general observation scheme, the datum and configuration problems are addressed, and having completed a detailed ZOD and FOD, the precision of the network is examined. If the specifications for an ideal $Q_x^{(2)}$ are met and/or if the network is deemed to be optimal, the design is complete. Should the simulated network fail the test of optimality with respect to the specified accuracy criteria, then the question of whether meeting specifications is a matter of scaling $Q_x^{(2)}$ should be asked. If such an approach is practicable, the SOD process (multiple exposures and/or multiple image coordinate measurements) can be followed until an optimal network precision is obtained.

If the structure of $Q_x^{(2)}$ (e.g., its lack of homogeneity) causes the network to fail the test of optimality, then the SOD is bypassed and either the network design is revised, principally through the FOD process, or the general observation and measuring scheme are completely redesigned. In practice, this whole procedure can be carried out interactively at the computer terminal.

CONCLUDING REMARKS

This paper has dealt with the optimization of design of photogrammetric networks, and the interconnected processes of zero-, first-, second-, and third-order design have been outlined. Also, through the use of a number of simulated networks, some salient general features relating design and precision have been illustrated. From the treatment of the different design classifications outlined, it should not be implied that photogrammetric network optimization amounts to a formal step-by-step procedure through ZOD, FOD, and SOD. The flow diagram presented in Figure 3 describes one general scheme, but more often than not other factors such as previous experience and intuition will play a central role in network optimization. In any computer simulation, however, it is useful to keep in mind the general design characteristics discussed.

REFERENCES

- Ackermann, F., 1981. Reliability and Gross Error Detection in Photogrammetric Blocks. *Deutsche Geodätische Kommission, Series B, No. 258/V, pp.49-67.*

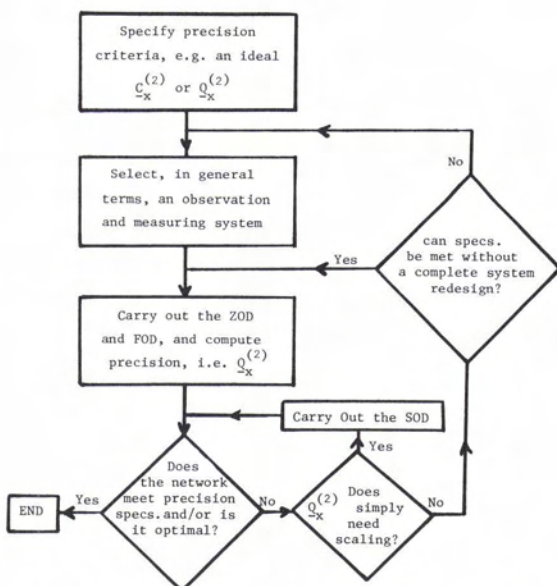


FIG. 3. Flow diagram for photogrammetric network design optimization.

- Alberda, J. E., 1980. A Review of Analysis Techniques for Engineering Control Schemes. *Proceedings of the Industrial and Engineering Survey Conference*, London.
- Baarda, W., 1973. S-Transformations and Criterion Matrices. *Netherlands Geodetic Commission, Publ. on Geodesy*, Vol. 5, No. 1.
- Blaha, G., 1971. *Inner Adjustment Constraints with Emphasis on Range Observations*. Dept. of Geodetic Science Report No. 148, Ohio State University, Columbus, 85 p.
- Brown, D. C., 1980. *Application of Close-Range Photogrammetry to Measurements of Structures in Orbit*. GSI Technical Report No. 80-012, Geodetic Services Inc., Melbourne, Florida, Vol. 1, 131 p.
- , 1982. STARS, A Turnkey System for Close-Range Photogrammetry. *International Archives of Photogrammetry*, Vol. 24, Part V/1, pp. 68-89.
- Cross, P. A., 1981. Report of SSG 1.59: Computer Aided Design of Geodetic Networks. *Deutsche Geodätische Kommission*, Series B, No. 258/III, pp. 13-21.
- El-Beik, A. H., and R. Babaei-Mahani, 1982. Quadrastational Close-Range Photogrammetric System. *International Archives of Photogrammetry*, Vol. 24, Part V/1, pp. 129-143.
- Förstner, W., and R. Schroth, 1981. On the Estimation of Covariance Matrices for Photogrammetric Image Coordinates. *Deutsche Geodätische Kommission*, Series B, No. 258/VI, pp. 43-70.
- Fraser, C. S., 1980. Multiple Focal Setting Self-Calibration of Close-Range Metric Cameras. *Photogramm. Eng. Remote Sensing*, Vol. 46, pp. 1161-1171.
- , 1982. Optimization of Precision in Close-Range Photogrammetry. *Photogramm. Eng. Remote Sensing*, Vol. 48, pp. 561-570.
- , 1983. Photogrammetric Monitoring of Turtle Mountain: A Feasibility Study. *Photogramm. Eng. Remote Sensing*, Vol. 49, pp. 1551-1559.
- Gates, J. W. C., S. Oldfield, C. Forno, P. J. Scott, and S. A. Kyle, 1982. Factors Defining Precision in Close-Range Photogrammetry. *International Archives of Photogrammetry*, Vol. 24, Part V/1, pp. 185-195.
- Grafarend, E. W., 1974. Optimization of Geodetic Networks. *Bolletino di Geodesia a Science Affini*, Vol. 33, No. 4, pp. 351-406.
- Grafarend, E. W., H. Heister, R. Kelm, H. Kropff, and B. Schaffrin, 1979. *Optimierung Geodätischer Meßoperationen*. Wichmann-Verlag, Karlsruhe, 500 p.
- Granshaw, S. E., 1980. Bundle Adjustment Methods in Engineering Photogrammetry. *Photogrammetric Record*, Vol. 10, No. 56, pp. 181-207.
- Grün, A., 1978. Accuracy, Reliability and Statistics in Close-Range Photogrammetry. *Presented Paper, Symposium of ISP, Comm. V.*, Stockholm, August.
- , 1980. Precision and Reliability Aspects in Close-Range Photogrammetry. *Invited Paper, XIV Congress of ISP, Comm. V.*, Hamburg, July.
- Hottier, P., 1976. Accuracy of Close-Range Analytical Restitutions: Practical Experiments and Prediction. *Photogramm. Eng. Remote Sensing*, Vol. 42, pp. 345-375.
- Kenfick, J. F., 1971. Ultra-precise Analytics. *Photogramm. Eng.*, Vol. 37, pp. 1167-1187.
- Mephram, M. P., and E. J. Krakiwsky, 1981. Interactive Network Design and Analysis. *Deutsche Geodätische Kommission*, Series B, No. 258/III, pp. 90-96.
- Niemeier, W., 1982. Design, Diagnosis and Optimization of Monitoring Networks in Engineering Surveying. *Presented Paper, The Centennial Convention of CIS*, Ottawa.
- Papo, H., and A. Perelmuter, 1982. Free Net Analysis in Close-Range Photogrammetry. *Photogramm. Eng. Remote Sensing*, Vol. 48, pp. 571-576.
- Schmitt, G., 1981. Optimal Design of Geodetic Networks. *Deutsche Geodätische Kommission*, Series B, No. 258/III, pp. 7-12.
- Schwartz, D., 1982. Close-Range Photogrammetry for Aircraft Quality Control. *Proceedings of ASP Annual Meeting*, Denver, pp. 353-360.
- Strang Van Hees, G. L., 1982. Variance-Covariance Transformations of Geodetic Networks. *Manuscripta Geodaetica*, Vol. 7, pp. 1-20.
- Torlegård, K., 1980. On Accuracy Improvement in Close-Range Photogrammetry. *Proceedings of the Industrial and Engineering Survey Conference*, London.
- Veress, S. A., and J. N. Hatzopoulos, 1981. A Combination of Aerial and Terrestrial Photogrammetry for Monitoring. *Photogramm. Eng. Remote Sensing*, Vol. 47, pp. 1725-1731.

(Received 28 January 1983; accepted 11 March 1984)

Forthcoming Articles

The September 1984 issue of the Journal will celebrate the Fiftieth Anniversary of the American Society of Photogrammetry with articles describing some of the early pioneers of photogrammetry and highlighting milestones and events in photogrammetry and remote sensing in this country.